

How well do domain wall fermions realize chiral symmetry?

George R. Fleming * ^a

^aPhysics Dept., Columbia University, New York NY 10027

In the domain wall fermion formulation, chiral symmetry breaking in full QCD is expected to fall exponentially with the length of the extra dimension. We measure the chiral symmetry breaking due to a finite extra dimension in two ways, which can be affected differently by finite volume and explicit fermion mass. For quenched QCD the two methods generally agree, except for the largest extent of the extra dimension, which makes the limit uncertain. We have less data for full QCD, but see exponential suppression for the method where we have data.

1. Introduction

Lattice QCD with massless domain wall fermions (including fermion loop effects) [1][2] is expected to have the $SU_L(N_f) \otimes SU_R(N_f)$ chiral symmetry of the continuum when the extent of the extra dimension, L_s , becomes infinite. For simulations, where the volume is finite and particles are not strictly massless, reliable techniques are needed to quantify the symmetry breaking for finite L_s . Such techniques are needed to see the expected $\exp(-\alpha L_s)$ dependence of chiral breaking for full QCD and determine if this is also the case for the quenched theory.

Here we report results from two techniques for measuring chiral symmetry breaking due to finite L_s ; the first uses the pion mass and the second the axial Ward identity. At zero temperature, the pion mass is governed by the axial Ward identity. However, in simulations with finite volume and with finite quark masses, it is important to check the agreement between these approaches.

The axial Ward identity is the origin of the Gell-Mann-Oakes-Renner (GMOR) relation, discussed previously for domain wall fermions in [3]. The fermion action of [2] is used, with the modifications of [4]. Some details on the numerical methods are in [5]. See [6] for a general review on domain wall fermions and references.

2. m_{res} for domain wall fermions

If the dominant effect of finite L_s is to produce an extra contribution, m_{res} , to the total quark mass, then one would expect

$$m_\pi^2 = c_0(V) + c_1(V) * (m_f + m_{\text{res}}) + \dots \quad (1)$$

where V is the space-time volume and it is expected that $c_0(V) \rightarrow 0$ as $V \rightarrow \infty$. For finite volume, a result we call $m_{\text{res}}^{(m_\pi^2)}$, can be found from $m_\pi^2(m_f = 0)/c_1(V)$, which is m_{res} when $c_0(V) = 0$.

Using the flavor non-singlet axial current in [2] we integrate the axial Ward-Takahashi identity to get

$$\langle \bar{q}_0 q_0 \rangle = m_f \chi_\pi + \Delta J_5 \quad (2)$$

where the pseudoscalar susceptibility is (no sum on a)

$$\chi_\pi \equiv 2 \sum_x \left\langle \bar{q}_x \gamma_5 \frac{\lambda^a}{2} q_x \bar{q}_0 \gamma_5 \frac{\lambda^a}{2} q_0 \right\rangle, \quad (3)$$

the additional contribution from chiral mixing due to finite L_s is

$$\Delta J_5 \equiv 2 \sum_x \left\langle j_5^a(x, L_s/2) \bar{q}_0 \gamma_5 \frac{\lambda^a}{2} q_0 \right\rangle, \quad (4)$$

and q_x are four-dimensional fermion fields defined from the appropriate right- and left-handed fields at the boundaries of the extra dimension.

For large volumes in the chirally broken phase, the pseudoscalar susceptibility is expected to behave as

$$\chi_\pi = a_{-1}/(m_f + m_{\text{res}}) + a_0 + \mathcal{O}(m_f + m_{\text{res}}). \quad (5)$$

*In collaboration with P. Chen, N. Christ, A. Kaehler, T. Klassen, C. Malureanu, R. Mawhinney, G. Siegert, C. Sui, P. Vranas, L. Wu, Y. Zhestkov. Supported in part by DOE grant # DE-FG02-92ER40699 and in part by NSF grant # NSF-PHY96-05199 (PMV).

The first term again says that, for large volumes, the pion is massless at $m_f = -m_{\text{res}}$, while a_0 gives the contribution due to the massive modes. Clearly, the pion pole contribution only dominates for large enough volumes and small enough $m_f + m_{\text{res}}$.

$j_5^a(x, L_s/2)$, a pseudoscalar density located midway between the domain walls, also has a pole contribution, whose coefficient is suppressed by propagation from $L_s/2$ to the boundaries. Since χ_π and ΔJ_5 both have a pole at $m_f = -m_{\text{res}}$ and when the pole terms dominate (2) $\langle \bar{q}_0 q_0 \rangle$ is finite, we can write in general

$$\Delta J_5 = m_{\text{res}} \chi_\pi + b_0 + \mathcal{O}(m_f + m_{\text{res}}). \quad (6)$$

We define $m_{\text{res}}^{(\text{GMOR})}$ by simultaneously fitting to the form

$$\langle \bar{q}_0 q_0 \rangle = (m_f + m_{\text{res}}) \chi_\pi + b_0. \quad (7)$$

and χ_π as given in (5). For a given L_s , this is a four parameter fit for a_{-1}, a_0, b_0 and $m_{\text{res}}^{(\text{GMOR})}$. Note that only if b_0/χ_π is small, can we get a reliable estimate for $m_{\text{res}}^{(\text{GMOR})}$ from $\langle \bar{q}_0 q_0 \rangle / \chi_\pi - m_f$. For full QCD, both $m_{\text{res}}^{(\text{GMOR})}$ and b_0 should approach zero exponentially in L_s , since both involve propagation from $L_s/2$ to the walls.

3. m_{res} in quenched QCD

We first find $m_{\text{res}}^{(m_\pi^2)}$ for the the $\beta = 5.7$, $m_0 = 1.65$, $8^3 \times 32$ quenched domain wall spectrum study we reported last year [7]. For quenched QCD, the observed zero mode contribution to $\langle \bar{q}_0 q_0 \rangle$ is small for $m_f \geq 0.02$, so we restrict our attention this mass range here. Figure 1, shows $m_{\text{res}}^{(m_\pi^2)}$ for our $\beta = 5.7$, $m_0 = 1.65$, $8^3 \times 32$ simulations from a correlated, linear fit of m_π^2 to valence masses 0.02, 0.06, 0.10, with errors from jackknifing. The $L_s = 32$ and 48 values are the same within errors, making the large L_s limit seem non-zero. For $L_s = 24$ the result for a $16^3 \times 32$ lattice is also shown, revealing that finite volume effects are noticeable.

Figure 1 also shows $m_{\text{res}}^{(\text{GMOR})}$ from a correlated fit to (7) and (5). The 16^3 GMOR point is on top of the 8^3 point in the plot. The fits $m_{\text{res}} = 0.059(14) \exp[-0.052(10)L_s]$ and $b_0 =$

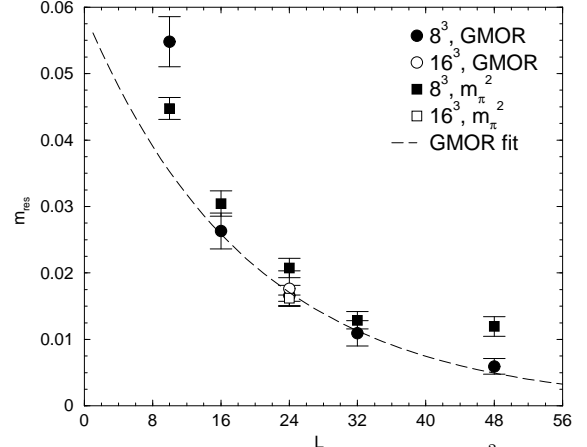


Figure 1. Comparison of $m_{\text{res}}^{(m_\pi^2)}$ and $m_{\text{res}}^{(\text{GMOR})}$ at quenched $\beta = 5.7$

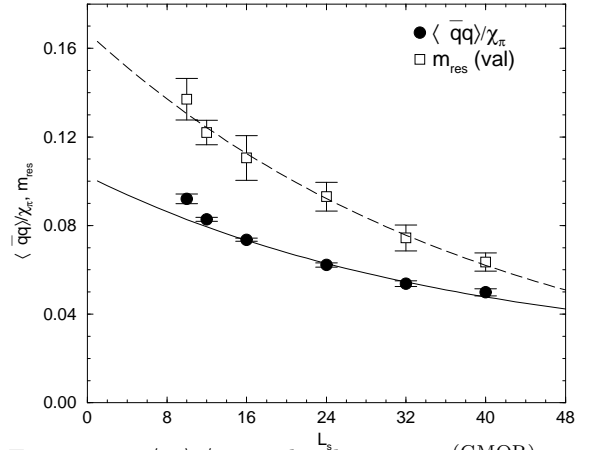


Figure 2. $\langle \bar{q}q \rangle / \chi_\pi$ and valence $m_{\text{res}}^{(\text{GMOR})}$ on $8^3 \times 4$, $\beta = 5.2$, $m_0 = 1.9$, $m_f = 0.02$ lattices.

$-0.0035(11) \exp[-0.051(13)L_s]$ (not shown) are consistent with ΔJ_5 vanishing in the $L_s \rightarrow \infty$ limit.

The agreement between the two methods for $L_s \leq 32$ is reasonable and only occurs since b_0 is included in the fits. $m_{\text{res}}^{(\text{GMOR})}$ is volume independent for $L_s = 24$, while $m_{\text{res}}^{(m_\pi^2)}$ is not. The discrepancy for $L_s = 48$ may be due to finite volume, but needs further study.

4. m_{res} in $N_f = 2$ QCD

For full QCD, we have done extensive simulations with the Wilson gauge action and do-

Table 1

Valence m_{res} comparison on $8^3 \times 32$ lattices

L_s	m_f	$m_{\text{res}}^{(m_\pi^2)}$	$m_{\text{res}}^{(\text{GMOR})}$	$-b_0$
Wilson gauge action, $\beta = 5.325, m_0 = 1.9$				
24	0.02	0.0622(9)	0.058(2)	0.0047(3)
	0.06	0.0645(6)	0.059(2)	0.0046(2)
Iwasaki gauge action, $\beta = 1.9, m_0 = 1.9$				
24	0.02	0.0401(5)	0.038(2)	0.0028(2)
Iwasaki gauge action, $\beta = 2.0, m_0 = 1.9$				
24	0.02	0.0158(9)	0.015(2)	0.0013(3)
	0.06	0.019(1)	0.017(3)	0.0015(4)
48	0.02	0.0073(16)	0.011(2)	0.0010(2)

main wall fermions on $8^3 \times 4$ volumes for several values of L_s with $\beta = 5.2$, $m_0 = 1.9$ and $m_f = 0.02$. For these lattices, which are in the low temperature phase, we show $\langle \bar{q}q \rangle / \chi_\pi$ in Figure 2. An exponential fit, yielding $\langle \bar{q}q \rangle / \chi_\pi = 0.02 + 0.082(3) \exp[-0.027(2)L_s]$ for $16 \leq L_s \leq 40$ with $\chi^2/N_{\text{dof}} = 2.76/2$, is also shown.

We have also done uncorrelated fits, using valence masses between 0.02 and 0.14, to extract $m_{\text{res}}^{(\text{GMOR})}$ and b_0 , since for the dynamical simulations there is not enough data to resolve the covariance matrix. (For the quenched case there was little difference between the correlated and uncorrelated fits.) All fits have $N_{\text{dof}} = 4$ and $\chi^2/N_{\text{dof}} \lesssim 1$. $m_{\text{res}}^{(\text{GMOR})}$ is also shown in Figure 2 and the dashed line fit is $m_{\text{res}}^{(\text{GMOR})} = 0.17(2) \exp[-0.026(6)L_s]$ for $10 \leq L_s \leq 40$ with $\chi^2/N_{\text{dof}} = 0.35/4$. b_0 is not shown, but also fits the exponential form $b_0 = -0.0100(16) \exp[-0.0147(67)L_s]$ with $\chi^2/N_{\text{dof}} = 0.20/4$ over the same range in L_s .

In Table 1 we compare the two methods of extracting m_{res} using valence spectrum data from $N_f = 2$, $8^3 \times 32$ scale setting calculations [8]. All data was fit for $0.02 \leq m_f^{(\text{val})} \leq 0.1$. For the GMOR fit, $N_{\text{dof}} = 2$ and $\chi^2/N_{\text{dof}} \lesssim 1$ for all fits. We note that the two methods agree within statistics.

We can also calculate m_{res} both ways but with data as a function of the dynamical mass. Since there are only two dynamical masses, both methods are unconstrained so the errors quoted come from naive extrapolation. The results are summarized in Table 2.

Table 2

Dynamical m_{res} comparison on $8^3 \times 32$ lattices

β	$m_{\text{res}}^{(m_\pi^2)}$	$m_{\text{res}}^{(\text{GMOR})}$	$-b_0$
$m_0 = 1.9, L_s = 24$			
5.325	0.059(2)	0.053(7)	0.004(1)
2.0	0.013(2)	0.014(5)	0.0011(9)

5. Conclusions

We have gotten good agreement between $m_{\text{res}}^{(m_\pi^2)}$ and $m_{\text{res}}^{(\text{GMOR})}$ for a wide range of quenched and dynamical simulations by including the non-pole terms in the susceptibilities. From our current data, $m_{\text{res}}^{(\text{GMOR})}$ appears less volume dependent. For the quenched simulations at $L_s = 48$, the two methods do not agree, possibly as a result of finite volume effects. This case warrants further study.

Whether chiral symmetry is fully restored for quenched simulations in the $L_s \rightarrow \infty$ limit of domain wall fermions is still an open question. For $N_f = 2$ QCD, $m_{\text{res}}^{(\text{GMOR})}$ falls exponentially, even at quite strong coupling. The rate of chiral symmetry restoration is very slow leaving much room for improvement.

All numerical calculations were performed on the 400 Gflops QCDSF machine at Columbia and the 6 Gflops QCDSF machine at Ohio State.

REFERENCES

1. D.B. Kaplan, Phys. Lett. **B288**, 342 (1992) .
2. V. Furman and Y. Shamir, Nucl. Phys. **B439**, 54 (1995) .
3. G.R. Fleming *et al.*, Nucl. Phys. Proc. Suppl. **73**, 207 (1999) .
4. P.M. Vranas, Phys. Rev. **D57**, 1415 (1998) .
5. P.M. Vranas *et al.*, Nucl. Phys. Proc. Suppl. **73**, 456 (1999) .
6. T. Blum, Nucl. Phys. Proc. Suppl. **73**, 167 (1999) .
7. R. Mawhinney *et al.*, Nucl. Phys. Proc. Suppl. **73**, 204 (1999) .
8. L. Wu, these proceedings .
9. P.M. Vranas, these proceedings .